On the Role of Equatorial Ocean Modes in the ENSO Cycle*

Y. WAKATA** AND E. S. SARACHIK

Joint Institute for the Study of the Atmosphere and Ocean, University of Washington, Seattle, Washington

18 December 1989 and 24 September 1990

ABSTRACT

In order to test certain aspects of the ENSO mechanism proposed by Suarez and Schopf and by Battisti and Hirst, we force a shallow water ocean with 28 years of observed (FSU) winds and decompose both the atmospheric forcing and ocean response into equatorial modes.

The proposed mechanism was verified in the following sense. For each warm phase of the cycle, a downwelling Kelvin mode directly forced by the weakening of the trade winds in the central Pacific was found. The same wind anomaly forces an upwelling gravest Rossby mode which propagates freely westward and reflects as a freely propagating Kelvin mode at the western boundary. This Kelvin mode returns to the scene of the original warming and acts as a retarded forcing (of opposite sign) eventually switching the phase of the oscillation from warm to cold. The cold phase then proceeds, by the same mechanism but with modes of opposite signs, to eventually switch to the warm phase.

The contribution of the higher Rossby modes to this process is estimated. It is found that almost all the Kelvin response in the western Pacific results from the reflection of the gravest symmetric equatorial Rossby mode so that the ENSO cycle is defined by the interaction of only two ocean modes, the Kelvin and lowest Rossby mode. These modes are sometimes forced directly by the wind as part of an intrinsic coupled atmosphere–ocean mode and sometimes propagate freely where the wind forcing is negligible. The distinction between these two manifestations of the ocean modes is of the greatest importance and is stressed throughout the paper.

The case of the warm event of 1976 is an interesting example of the failure of the switching mechanism, and is discussed in the conclusion.

1. Introduction

The purpose of this note is the testing of the ENSO mechanism proposed by Suarez and Schopf (1988), Battisti (1988), and Battisti and Hirst (1989), using observed winds to force a shallow-water ocean model.

The proposed ENSO mechanism can be described as follows. A warm SST anomaly arises in the eastern and central Pacific by means of a local atmosphere–ocean instability. To the west, and in concert with the growing SST anomaly, westerly wind stress anomalies grow and reinforce the local unstable growth, primarily through the thermodynamic processes connected with a depressed thermocline forced by the westerly wind anomaly. Since the westerly wind anomalies are zonally confined, standard equatorial adjustment theory indicates that the thermocline will be raised at the western end of the wind anomalies and thereupon propagate westward, as free upwelling Rossby modes. These upwelling Rossby modes propagate westward, strike the western boundary, are reflected as freely propagating upwelling Kelvin modes, and return to the scene of the growing warm anomaly. At this point, evidence of free propagation ceases, and there is a continuing competition between the upwelling (therefore cooling) Kelvin mode, which continues to be forced (at a retarded time) by the instability, and the warming of the original local air–sea instability. Eventually the cooling Kelvin mode dominates and the original atmosphere–ocean instability is "switched" and the SST anomaly becomes cool. The entire cycle than proceeds into the cool phase, with exactly the same scenario but with all modes having opposite sign, until it again becomes warm. The ENSO is then viewed as a continuing cycle whose origin is a coupled instability and whose oscillatory properties are determined by the retarded forcing communicated by freely propagating equatorial modes.

How can we test this scenario? In his model ENSO cycle, Battisti (1988) was able to give precise meaning to the evolving phases of this cycle by diagnosing the model derived forcing and response in terms of equatorial modes. While it would be interesting to do this in the real ocean, there is neither enough data nor sufficiently precise data to make this possible, nor is there ever likely to be so. We therefore follow the best alternative and use the observed forcing fields for 28 years, a period that contains a number of warm and cold

* JISAO Contribution No. 68.

** Permanent Address: Faculty of Marine Science and Technology, Tokai University, Shimizu Shizuoka, Japan.

Corresponding author address: Dr. E. S. Sarachik, JISAO, AK-40, University of Washington, Seattle, WA 98195.

phases of the ENSO cycle, to force a linear shallow ocean model and diagnose the model ocean thermocline response in terms of equatorial modes.

It is important to note that, since we are decoupling the problem and forcing the shallow water ocean with *observed* winds, the underlying SST anomalies that produce this wind variability remain implicit. Thus, while the air–sea instability and the switching mechanism is intrinsically related to SST variability and therefore to the detailed thermodynamic mechanisms that change SST, explicit consideration of these processes is not required because they are correctly included in the variability of the observed winds. We set ourselves a simpler task, namely to see whether or not the forced and free equatorial ocean modes, as forced by the observed winds, are consistent with the ENSO mechanism described above.

It should also be noted that the experiment of forcing a shallow water model with long time series of observed winds has been performed many times (e.g., Busalacchi and O'Brien 1981; Busalacchi et al. 1983; Cane 1984; Kubota and O'Brien 1988; Zebiak 1989; Seager 1989) but none from the point of view of the modal response. Gill (1981) and Bigg and Blundell (1989) did similar experiments over very short time intervals characteristic of a single warm event and did decompose the forcing and response into modes: their results for their short intervals are consistent with ours.

In section 2 we briefly describe the model. In the third section, we discuss the modal decomposition of the atmospheric forcing fields, show the modal decomposition of the response, and discuss the reflections of the free modes at the western boundaries in order to discuss the role of the higher index Rossby modes. The note finishes with a discussion of the mechanism and a summary of our results.

2. Model description

The linear shallow water equations in the long-wave approximation (Gill 1980) are solved. The parameters of the model are the ones adopted by Zebiak and Cane (1987) and Battisti (1988), in particular, the mean thermocline depth is $H = 150$ m, the reduced gravity parameter is $g' = 5.6 \times 10^{-2}$ m s^{-2}, the first baroclinic mode speed is $C = 2.9$ m s^{-1}, the Newtonian and Raleigh friction parameters are $r^{-1} = 2.5$ year, and the parameter to convert wind to stress is $\rho C_D = 3.2 \times 10^{-3}$ kg m^{-3}. The ocean geometry is taken to be on a equatorial β plane and is rectangular in shape, extending from 29.75°S to 29.75°N and from 124°E to 80°W. The grid resolution is 0.5° latitude by 2° longitude and the time step is 10 days. The numerical scheme used is described in detail by Cane and Patton (1984).

The Florida State University pseudostress fields were used to force the ocean. They extend from January 1961 to June 1989 and are based on the subjectively interpolated ship winds compiled by Legler and O'Brien (1988). This wind set is a revised version, differing slightly from previous versions, in that part of the set has been augmented and reanalyzed using the COADS individual marine observations.

3. Results

The model was started from an initial motionless state by using the 1961 winds cyclically for 20 years to produce the initial annual climatology. The model was then run by imposing the winds from January 1961 to June 1989. The results are discussed in the following subsections.

a. *Thermocline depth*

The resulting thermal structure on the equator over the entire 28 years is shown in Fig. 1. In order to emphasize the interannual variability, a 12-month running mean filter has been applied to the thermal response and to all the other response fields.

The results are consistent with the other similar experiments referred to in the introduction (e.g., Busalacchi and O'Brien 1981; Busalacchi et al. 1983) and, in particular, the thermocline depressions characteristic of the warm events of 1962–63, 1965–66, 1972–73, 1976–77, 1982–83, and 1986–87 are clearly seen.

b. *Projections*

In order to interpret Fig. 1, we will decompose both the wind forcing and thermocline response into the equatorial modes of the system. Let us define F_n as the projection of the zonal wind

$$F_n(x) = \int \frac{\tau^{(x)}(x, y)}{\rho H} \Psi_n(y) dy \qquad (1a)$$

so that

$$\frac{\tau^{(x)}(x, y)}{\rho H} = \sum_n F_n(x) \Psi_n(y) \qquad (1b)$$

where

$$\Psi_n(y) = \pi^{-1/4}(2^n n!)^{-1/2} H_n(y) \exp\left(-\frac{y^2}{2}\right) \qquad (2)$$

is the normalized Hermite function.

Similarly, the ocean response, which we will examine in the Gill (1980) variable $S = u + h$, where h is the thermocline anomaly and u is the zonal current anomaly, is decomposed as

$$S(x, y) = \sum_n S_n(x) \Psi_n(y) \quad (n = 0, 1, 2, 3 \cdots). \qquad (3)$$

The amplitudes S_n of the response obey the following equations derived directly from the forced shallow water equations:

$$S_{0t} + S_{0x} = -rS_0 + F_0 \qquad (4a)$$

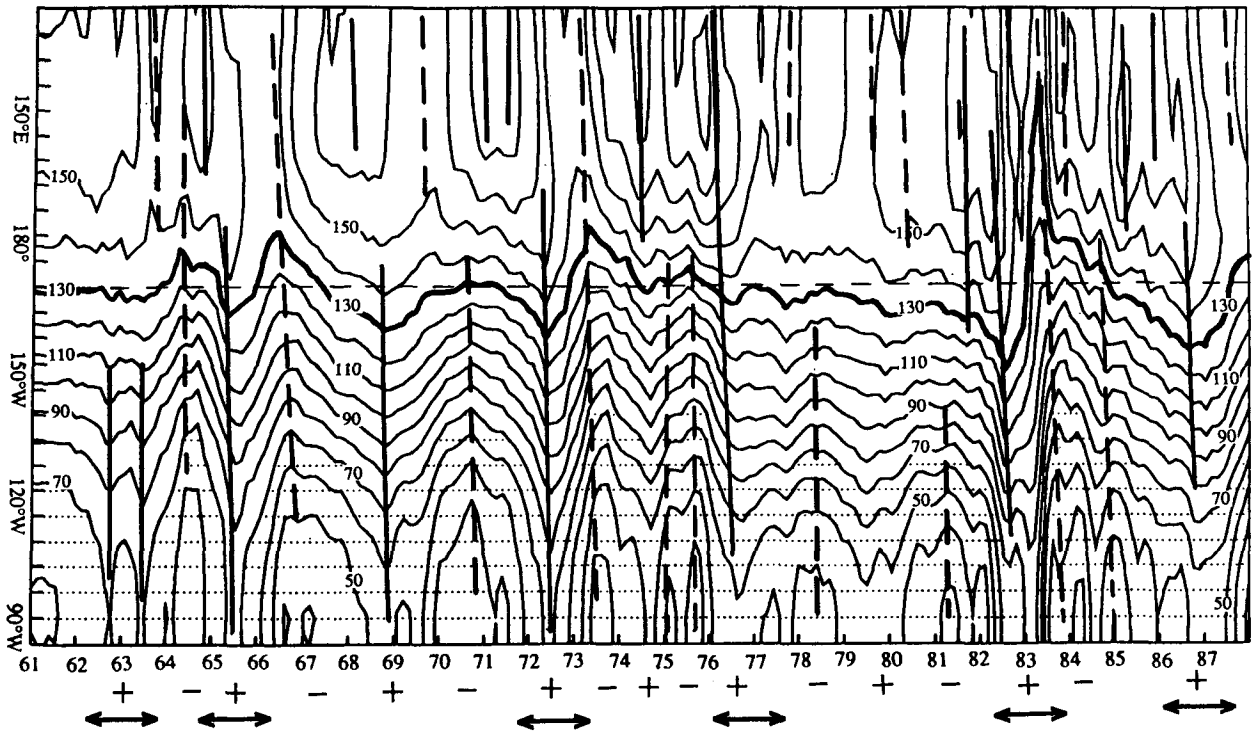

FIG. 1. The model thermal response on the equator. The area lower than 70 m is dotted. The contour interval is 10 m. Heavy straight lines show the peak of downwelling Kelvin mode, and dotted lines show upwelling Kelvin mode. The heavy curve shows the 130 m depth. Plus and minus marks below the abscissa indicate the direction of the air–sea coupled instability (see text).

and

$$S_{nt} - \frac{1}{(2n-1)} S_{nx} = -rS_n + \frac{(n-1)}{(2n-1)} F_n - \frac{(n^2-n)^{1/2}}{(2n-1)} F_{n-2} \quad (4b)$$

where Eq. (4b) holds for $n = 2, 3, 4, \cdots$.

c. *Wind forcing*

The projections of the zonal wind anomalies onto the Kelvin mode (F_0) and gravest symmetric Rossby mode $\frac{1}{3}(F_2 - 2^{1/2}F_0)$ are shown in Fig. 2. The values of the projections are nondimensionalized by C^2/L, where L is the equatorial length scale $(C/\beta)^{1/2}$.

The Kelvin projection (Fig. 2a) of the forcing is positive and strong in the central Pacific during the warm events of 1965–66, 1972–73, 1982–83, and 1986–87 but very weak during the peculiar warm event of 1976–77. A positive Kelvin forcing produces downwelling thermocline anomalies to the east of the forcing. During cold phases of the ENSO, the Kelvin forcing is negative and produces upwelling thermocline anomalies to the east of the forcing. Clearly the warm and cold phases of the ENSO occur in concert with the weakening and strengthening of the trade winds over the central Pacific. These wind stress anomalies may be considered as part of the atmosphere–ocean unstable mode that gets directly excited to form the ENSO. Since the forcing is spatially confined to the central Pacific, we may expect there to be a locally forced response that will be part of the coupled atmosphere–ocean mode, and a remote response consisting of free Kelvin modes propagating to the east of the wind forcing and free Rossby modes propagating off to the west.

The forcing of the gravest symmetric Rossby mode (S_2) is shown in Fig. 2b. This forcing has almost the same structure as the Kelvin forcing, but is of opposite sign. This may be understood mathematically by noting that the term F_0 is much larger than F_2 so that the forcing of S_2 is approximately $(-2^{1/2}/3)F_0$. This may be understood physically by noting that a confined positive wind forcing will force westward propagating modes of opposite sign than eastward propagating modes in order that the thermocline may adjust downward to the east of the positive forcing and upward to the west of the forcing.

The forcing is predominantly symmetric with respect to the equator so that the forcings of S_3 and higher odd modes are small. The higher symmetric forcings are similarly small compared to the forcing of the gravest symmetric mode and are therefore not shown.

d. *Modal ocean response*

Figures 3a–d shows respectively the response of the Kelvin mode S_0, the gravest symmetric Rossby mode

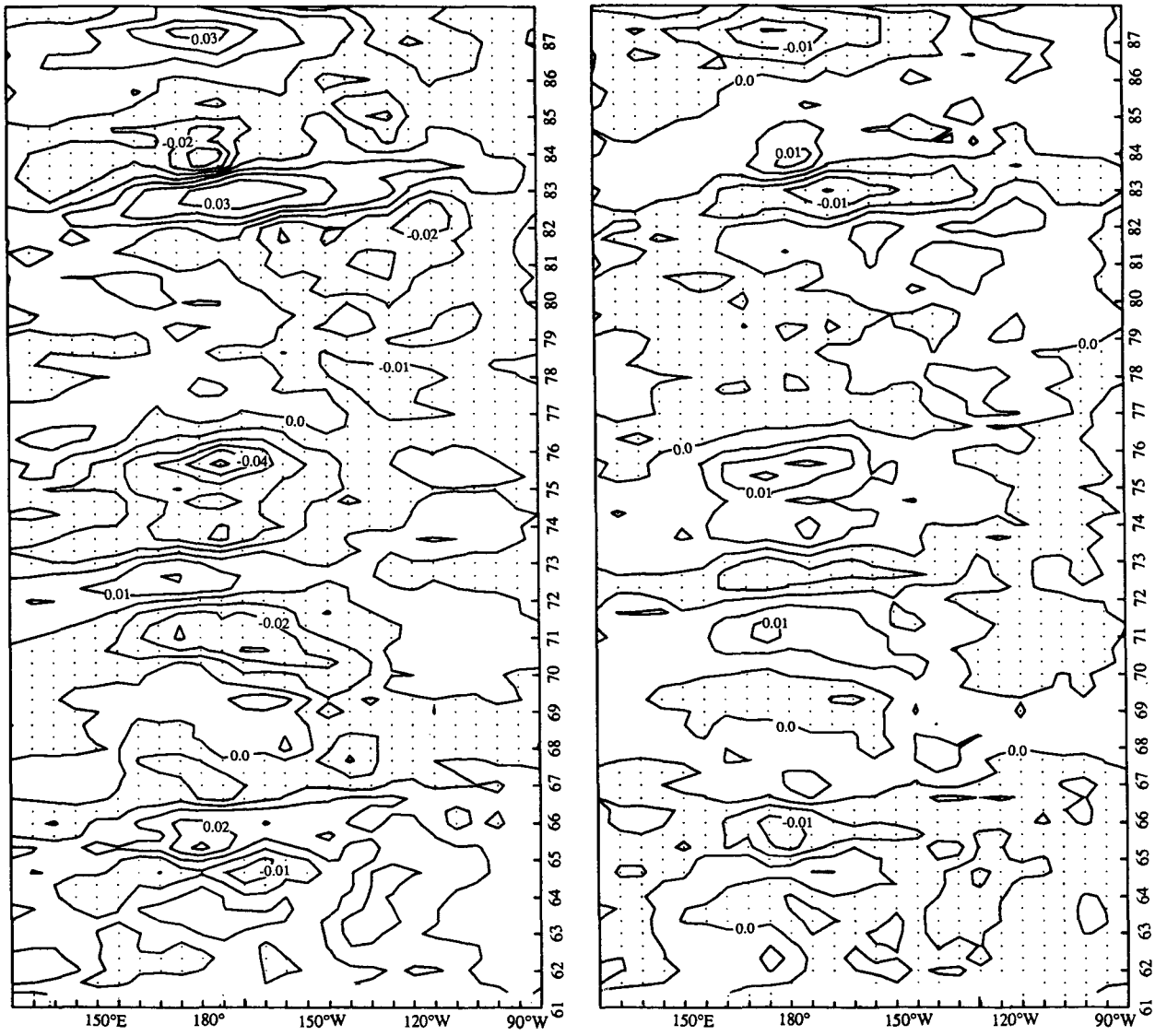

FIG. 2. (a) Anomaly of the Kelvin mode forcing. Negative area is dotted. Contour interval is 0.01. (b) Anomaly of the first symmetric equatorial Rossby mode S_2 forcing. Contour interval is 0.005.

S_2, the lowest anti-symmetric mode Rossby mode S_3, and the second symmetric Rossby mode S_4. The mixed Rossby gravity mode S_1 does not get excited in the long wave approximation. The free modal speeds are $C = 2.9$ m s^{-1} for the Kelvin mode, and $-C/(2n-1)$ for the Rossby modes. A free Kelvin mode would take 70 days to propagate across the entire basin. The peaks of thermocline anomaly associated with the $n = 2$ mode occur at 4°N and S, with $n = 3$ at 5.8°N and S, and with $n = 4$ at 7.2°N and S.

We see from Fig. 3a that during warm years, the downwelling Kelvin mode is excited and propagates eastward. (This Kelvin excitation is not present during the warm event of 1962–63 and its absence is probably an artifact of the initial spinup of the model). In order to aid our future discussion, the downwelling (upwelling) peaks of the Kelvin response of Fig. 3a are depicted by solid (dashed) lines in the total thermocline response of Fig. 1. We see that there are two separate sources for the Kelvin response: the western boundary and the region of the wind forcing. In general the Kelvin excitation due to these two sources do not line up. The Kelvin modes propagating eastward from the western boundary meet the region of wind forcing of opposite sign. Not until the wind forcing region switches sign will Kelvin modes of the same sign that left the western boundary also be forced from the wind forcing region and propagate eastward.

Figure 3b shows the gravest symmetric Rossby response, S_2. In the central part of the basin, the response

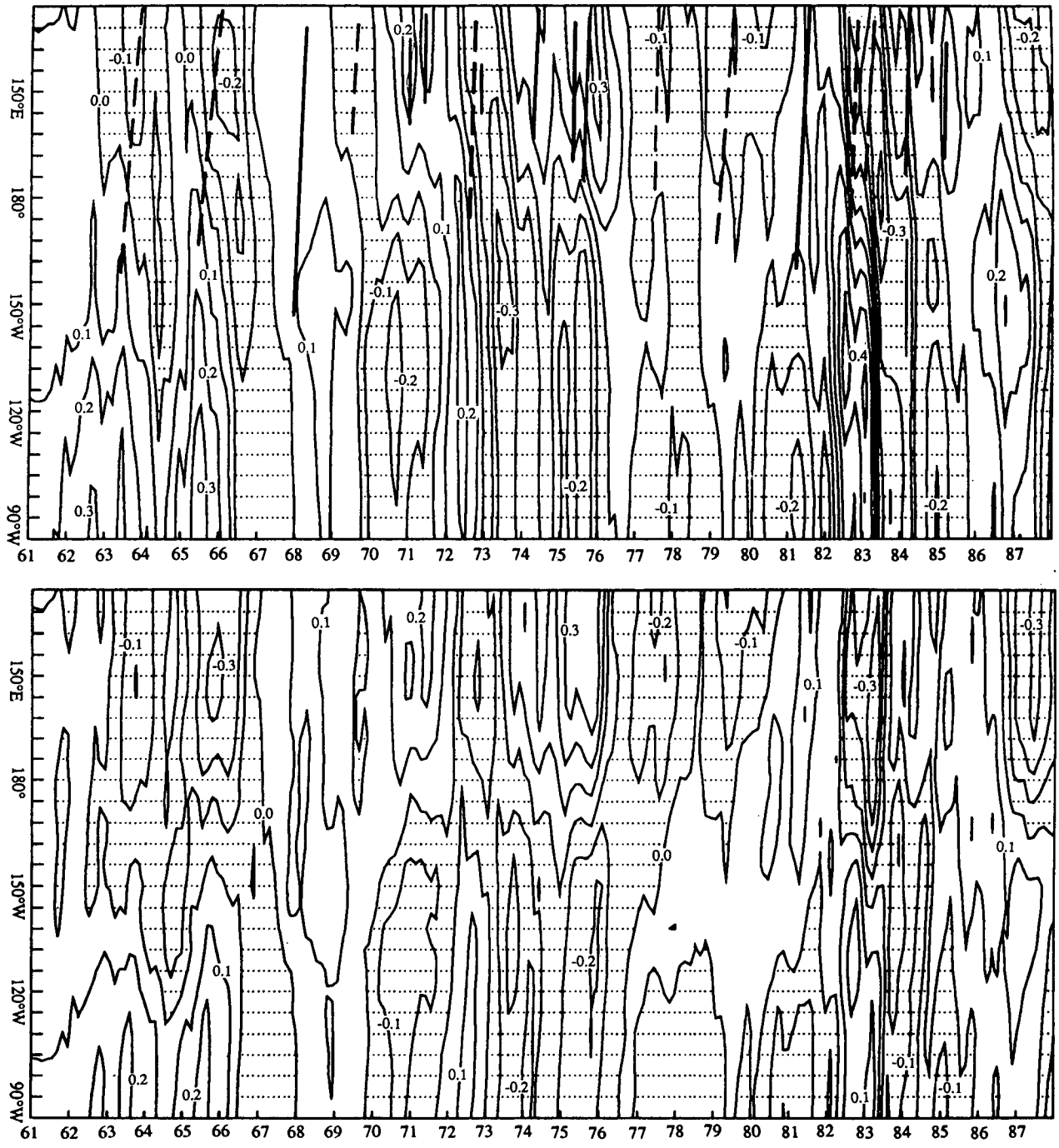

FIG. 3. (a) Anomaly of Kelvin wave amplitude. Dotted area shows upwelling. Heavy lines show the peak of downwelling equatorial Rossby wave S_2. Dashed lines show the upwelling equatorial Rossby wave. The contour interval is 0.1. (b) Same as (a) but the first symmetric equatorial Rossby wave S_2. (c) Same as (a) but the first antisymmetric equatorial Rossby wave S_3. (d) Same as (a) but the second symmetric equatorial Rossby wave S_4.

tends to follow the forcing (Fig. 2b) and is therefore part of the direct coupled atmosphere–ocean mode. However, westward propagation is clearly evident in the western Pacific; this is characteristic of free propagating modes. The westward propagating upwelling (downwelling) peaks evident in Fig. 3b are transcribed to Fig. 3a as dashed (solid) lines.

It is now clear from Fig. 3a that about one year prior to each warm event, a downwelling freely propagating Rossby mode (solid line in Fig. 3a) was present in the

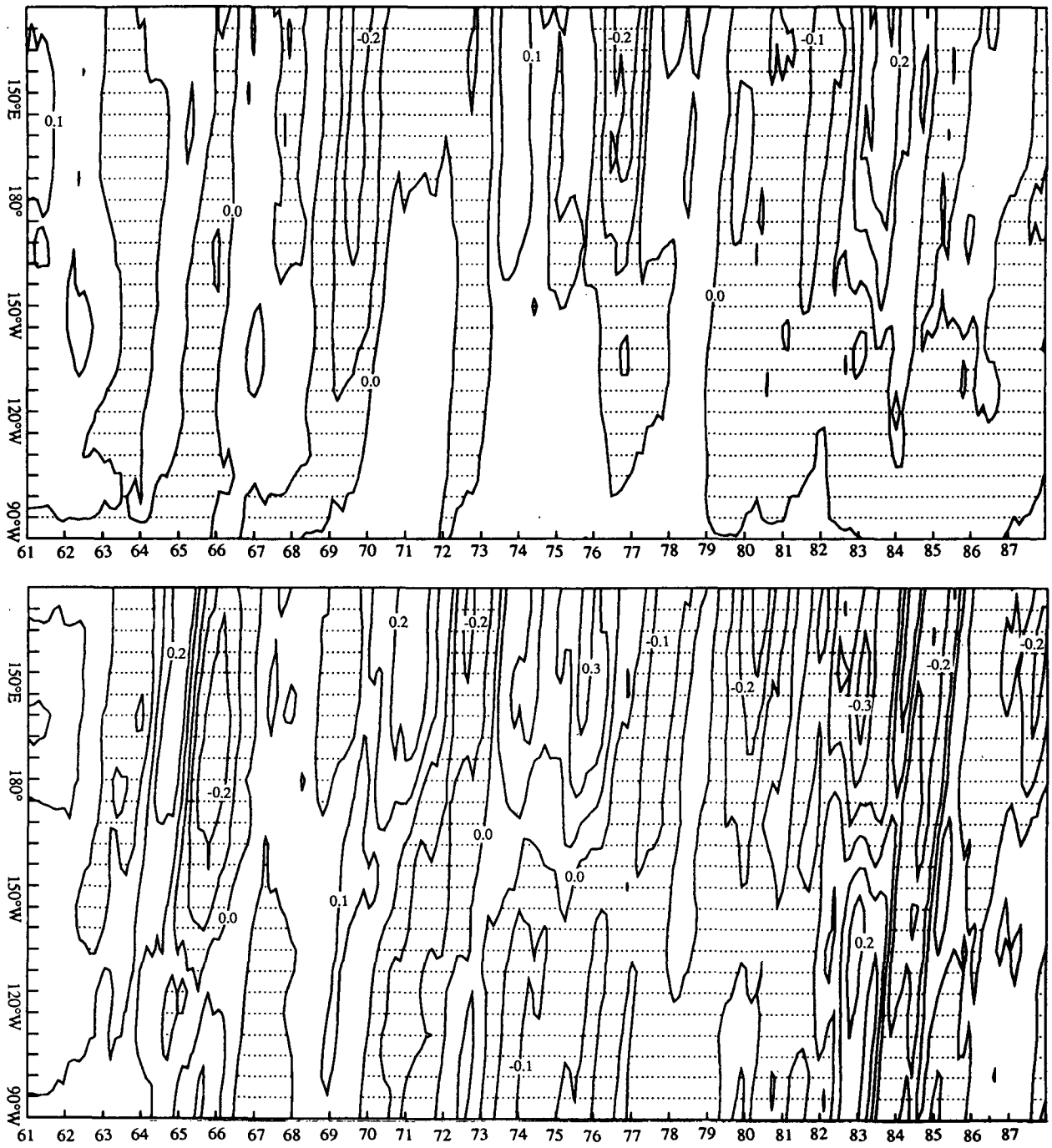

FIG. 3. (*Continued*)

western Pacific. Similarly, before a cold event, an upwelling freely propagating Rossby mode (dashed line in Fig. 3a) was present in the western Pacific. The downwelling Rossby mode connects to a downwelling Kelvin mode in the western Pacific by the process of reflection, but this reflected downwelling Kelvin mode does not directly connect to the Kelvin mode that produces the warm water in the eastern Pacific characteristic of warm events. This is most obvious in Fig. 3a for the warm events of 1968–69, 1972–73, and 1986–87.

The reflected freely propagating Kelvin modes in the western Pacific can be traced as far east as the date line. The downwelling Kelvin mode characteristic of the warm event is emitted from the central Pacific

about a year after the arrival of the freely propagating downwelling Kelvin mode produced by reflection at the western boundary. Similarly, the upwelling Rossby modes reflect as upwelling Kelvin modes, which propagate freely into the central Pacific, but the upwelling Kelvin modes characteristic of cold events do not appear until about a year after the arrival of the freely propagating Kelvin mode from the west.

This is completely consistent with the ENSO scenario of Suarez and Schopf (1988), Battisti (1988) and Battisti and Hirst (1989) described in section 1. The Kelvin modes characteristic of the warm events are part of forced response from the unstable coupled atmosphere–ocean mode. The Kelvin modes arriving from the western boundary are freely propagating (there is very little wind forcing present in the west Pacific, Fig. 2a) and are the result of reflections of freely propagating Rossby modes. The freely propagating downwelling Kelvin modes reach the central Pacific when the thermocline anomalies there are negative, i.e., cold conditions are still present. The downwelling signal delivered by the incoming Kelvin mode from the west is the result of the same cold event which sent downwelling Rossby signals to the western boundary. The downwelling Kelvin signal is therefore the retarded forcing of the cold event, acting at a retarded time given by the free propagation time of the Rossby mode and its reflected Kelvin mode. The retarded downwelling Kelvin signal now works, through the thermodynamic effect of downwelling on SST, to gradually warm the central Pacific. When the SST in the eastern and central Pacific switches from cold to warm, a warm coupled instability now grows and the resulting emitted Kelvin mode then grows in the eastern Pacific.

These downwelling Kelvin modes characteristic of warm events reflect at the eastern boundary and propagate westward as Rossby modes. The lowest Rossby mode S_2 does not make it back to the western Pacific because it meets the opposed wind forcing from the western edge of the forcing region (Fig. 3b). The next symmetric Rossby mode S_4 does make it back from the eastern boundary to the west (Fig. 3d), partly because the wind forcing is so narrowly confined latitudinally that it offers little forcing to the mode and partly because its slow speed brings it back to the forcing region at a time when the forcing has already switched to enhance this mode.

The first antisymmetric Rossby mode S_3 is shown in Fig. 3c. Negative amplitude modes are produced directly by the winds in all the warm years except 1982–83, but their amplitudes are small. Because the symmetry is wrong, they cannot be produced by the reflection of Kelvin modes at the eastern boundary nor can they produce Kelvin modes upon reflection at the western boundary.

e. Reflection of Rossby modes at the western boundary

Examination of Figs. 3a and 3b shows that the freely propagating Kelvin mode in the western Pacific seems to be produced by the reflection of the S_2 Rossby mode but, upon examining Fig. 3d, it also appears to be related to the reflection of the S_4 mode. (There is some asymmetric Rossby mode excitation as we see from Fig. 3c, but since asymmetric modes cannot reflect into Kelvin modes, we will not consider the asymmetric Rossby mode further). We can evaluate the relative importance of the various modes by examining the reflection relation between the Kelvin amplitude S_0 and the amplitudes S_n of the Rossby modes (Cane and Sarachik 1981; Hirst 1988) as follows:

$$S_0(x=0) = \sum_n \left(\frac{n-1}{n}\frac{n-3}{n-2}\cdots\frac{1}{2}\right)^{1/2} \times (n-1)^{-1}\cdot S_n(0). \quad (5)$$

Using Eq. (5), we see that the contribution to S_0 of a unit amplitude in S_2 is 0.71, to a unit amplitude in S_4 is 0.20, and to a unit amplitude in S_6 is 0.11. Figure 4 shows the contributions from the Rossby modes and the amplitude of the Kelvin mode at 150°E. We see that the response in the western Pacific can primarily be explained by the reflection of the gravest symmetric Rossby mode, S_2. Neither the wind forcing in this region nor the reflection of the higher Rossby modes are effective in forcing the freely propagating Kelvin mode near the western boundary.

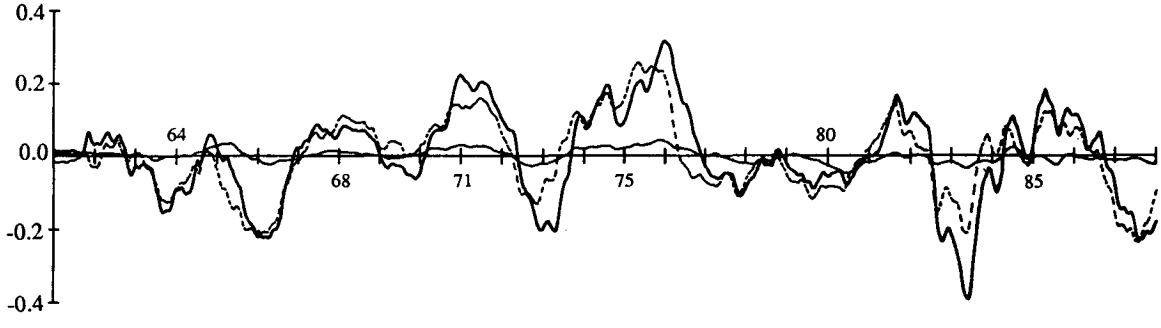

FIG. 4. Heavy solid line is the amplitude of the Kelvin mode at 150°E, dashed line is a contribution to Kelvin mode from S_2 mode and thin solid line is a contribution from S_4 mode.

There has been some controversy on this point in the literature. White et al. (1985, 1989) argue for the importance of the higher Rossby modes. They show a time versus longitude map of vertically averaged temperature anomaly at 12°N (White et al. 1989, Fig. 4) which shows positive anomalies appearing in 1982 and 1984 in the western Pacific. These anomalies can be traced from the small 1979–80 event and the 1982–83 event in the eastern Pacific, respectively. The warm anomaly from the east in 1982 connects directly to the subsequent eastward propagating anomaly; while in 1984, the eastward propagating anomaly appears one year after the arrival of the westward propagating anomaly and is clearly of the wrong sign to produce the Kelvin mode. Note that the 12°N anomalies look very much like our S_4 results, but since our S_4 peaks at 7.2°N, this result must be fortuitous.

In our Fig. 4, S_4 is positive in 1982 and 1984. The arrival of the positive anomaly S_4 connects to the peak of the Kelvin mode in 1982, but in 1984 the dominant peak of the Kelvin mode appears a full year after the S_4 anomaly. It is clear that the peak of the reflected Kelvin mode in 1985 resulted not from the arrival of S_4, which is the wrong sign, but from the gravest mode S_2.

We should note that there will always be amplitude in S_4 during the ENSO cycle since it is produced by the Kelvin mode at the eastern boundary. Using Hirst (1988), we find that a unit amplitude Kelvin mode at the eastern boundary will, on reflection, produce S_4 of amplitude 0.61, but at the western boundary a unit S_4 will, on reflection, only produce a Kelvin amplitude of 0.20.

We can summarize by saying that almost all of the Kelvin response in the western Pacific is produced by reflection of the gravest equatorial Rossby mode, in agreement with the modeling work of Battisti (1989) and the recent observational work of Kessler (1990).

4. Discussion and conclusion

The forcing and response of an ocean model using observed winds were discussed in this paper. It was pointed out that the modal responses are consistent with understanding the ENSO cycle as an atmosphere–ocean instability switched from phase to phase by the thermodynamics accompanying the retarded signaling due to propagating equatorial modes.

The key feature in this scenario is that the wind anomalies in the central Pacific are produced by SST anomalies in the eastern Pacific as a result of unstable growth of a coupled mode. Since the wind anomalies are both latitudinally and longitudinally confined, there will be a directly forced thermocline response only in the local region of the wind anomalies. According to equatorial adjustment theory, this direct response has opposite signs at the eastern and western ends of the forcing region: a positive (westerly) anomaly will lower the thermocline at the eastern end of the forcing region and raise it at the west. The responses then travel eastward as a freely propagating downwelling Kelvin mode and westward as a series of freely propagating upwelling Rossby modes, although in practice, only the gravest Rossby mode need be considered.

The warm unstable growth is eventually reversed by the action of the westward propagating Rossby mode which reflects at the western boundary as a returning Kelvin mode with a sign (upwelling) to oppose the original unstable growth. There will be a time $O(1\ \text{yr})$ when the returning upwelling Kelvin mode and the instability are opposing each other. After the Kelvin mode switches the instability, the cold instability grows and an upwelling Kelvin mode is emitted to the east (cooperating with the cold phase) and a downwelling Rossby mode is emitted to the west. Thus as we see, it is not the Kelvin mode reflected at the western boundary that causes the cooling in the east; rather it is the Kelvin mode emitted from the instability. As we see in Fig. 1, the cycle is not periodic, but the same scenario of events happens for each warm and cold phase.

While we cannot simulate the underlying SST thermodynamics that drives this air–sea interaction with our simple model, we have verified that the wave dynamics are consistent with this scenario for both warm and cold phases of the ENSO. In lieu of SST, we take as a marker of the state of ENSO, the position of the 130 m depth contour at 168°W (in Fig. 1, the position of 168°W is shown by the horizontal dotted line and the 130 m depth is shown bold). When the 130 m contour shifts eastward of 168°W, we will denote the state as positive (this will correspond to a warm state). The sign of the state is shown by the series of plus and minus signs below the time axis of Fig. 1. When the depth moves through 130 m at this longitude, we will say that the thermodynamic state characterizing the air–sea interaction has switched. Indeed, inspection of Fig. 1 shows that warm events ($\leftrightarrow$) corresponding to + states are interleaved with cold events, corresponding to − states, with a period of about 3 years except for the period 1977–1981.

The warm event of 1976 is the peculiar event in this series. Instead of the warming Kelvin mode awaiting the switch of state, the event seems to be due directly to the propagation of a downwelling Kelvin mode all the way from the western boundary. The previous cold event in 1975 is very strong, and the depth of the upper layer in the eastern Pacific is quite shallow. The emitted downwelling Rossby mode and subsequently reflected downwelling Kelvin modes are both strong (Figs. 3a and 3b) and the returning Kelvin mode reaches the central Pacific at a time when the wind anomalies are weak. The Kelvin mode therefore meets little opposition and is able to propagate through to the eastern boundary and induce the warming directly. Indeed, examination of the wind forcing of the Kelvin mode in Fig. 2a shows no strong downwelling Kelvin forcing

(and therefore no strong Rossby forcing) in the central Pacific during 1976. The period after 1976 is anomalous in that it stays slightly warm but with no strong forcing or response until the advent of the 1982–83 event. The event of 1982–83 seems to exhibit the restarting of the coupled instability in the central Pacific after a long hiatus.

We can clarify the discussion still further and make closer contact with the results of Battisti's (1988) regular ENSO oscillation by compositing the major results

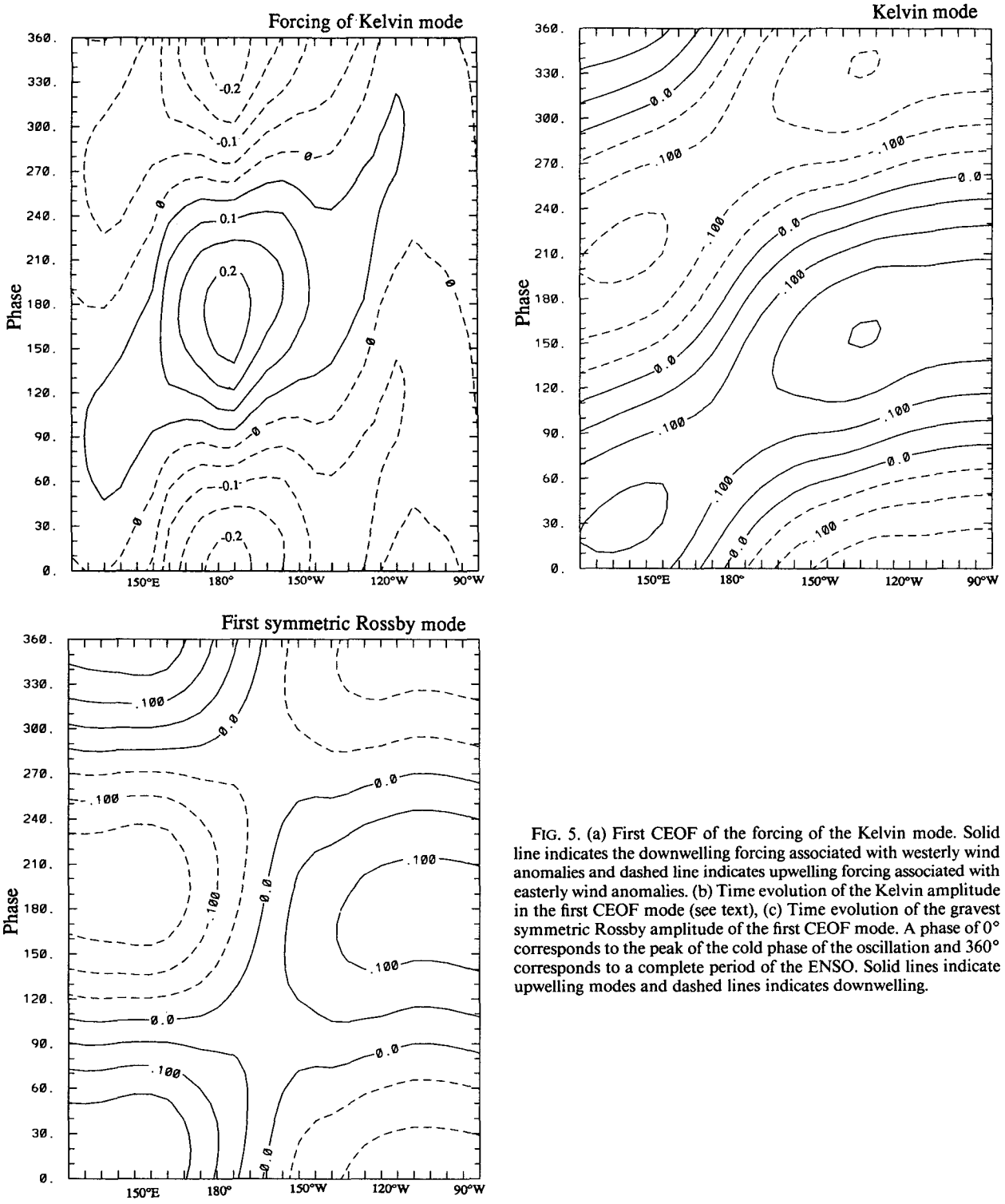

FIG. 5. (a) First CEOF of the forcing of the Kelvin mode. Solid line indicates the downwelling forcing associated with westerly wind anomalies and dashed line indicates upwelling forcing associated with easterly wind anomalies. (b) Time evolution of the Kelvin amplitude in the first CEOF mode (see text), (c) Time evolution of the gravest symmetric Rossby amplitude of the first CEOF mode. A phase of 0° corresponds to the peak of the cold phase of the oscillation and 360° corresponds to a complete period of the ENSO. Solid lines indicate upwelling modes and dashed lines indicates downwelling.

in Figs. 2 and 3 by means of a complex empirical orthogonal function (CEOF) method introduced by Barnett (1983) in which the modes of variation of a series consisting of three variables, the Kelvin mode forcing for the entire 28 year period and the Kelvin and Rossby responses over the same period, are found. The first CEOF of the combined series, with annual cycle removed, is the ENSO and explains 70% of the mutual variance of the original series. (Note that, in combining the variables, the forcing and responses were normalized by their spatially averaged standard deviations). A full cycle of 360° corresponds to a period close to 3 years. The Kelvin forcing part of the CEOF is shown in Fig. 5a (the Rossby forcing is the same but of opposite sign as explained in §3c) and the standardized responses of the Kelvin and gravest symmetric Rossby modes are shown in Figs. 5b and 5c.

We see clearly from this form of composite that the average ENSO cycle starts at the cold phase (0°) with negative Kelvin forcing (Fig. 5a) emitting an upwelling Kelvin mode eastward and downwelling Rossby mode westward (Figs. 5b and 5c). The Rossby amplitude reflects into a downwelling Kelvin mode (this is clear at phase 20°) and produced a weakening Kelvin upwelling response in the central Pacific until the Kelvin forcing reverses to positive (downwelling) at about 90° (Fig. 5a). The reinforced downwelling increases in the eastern Pacific until about 140° when the effect of the upwelling mode emitted from the western boundary at 130° starts to weaken the downwelling and eventually turns it to upwelling. The complete modal story is condensed into Fig. 5 and summarizes the role of the equatorial modes in the ENSO.

The fundamental cause of the ENSO is a coupled air–sea instability and the cause of the oscillatory behavior is the retarded forcing delivered by propagating equatorial modes propagating freely away from the region of wind forcing.

Acknowledgments. The authors would like to express their sincere thanks to Dr. D. Battisti for permitting the use of his ocean model and for valuable comments. Also, thanks are extended to Drs. O'Brien and Legler for providing the FSU wind data. This research was supported by a grant from the NOAA/EPOCS program and by a grant from the NOAA Office of Global Programs to the University of Washington Experimental Climate Forecast Center.

REFERENCES

Barnett, T. P., 1983: Interaction of the Monsoon and Pacific trade wind system at interannual time scales. Part I: The equatorial zone. *Mon. Wea. Rev.*, **111,** 756–773.

Battisti, D. S., 1989: On the role of off-equatorial oceanic Rossby waves during ENSO. *J. Phys. Oceanogr.*, **19,** 551–559.

——, 1988: Dynamics and thermodynamics of a warming event in a coupled tropical atmosphere–ocean model. *J. Atmos. Sci.*, **45,** 2889–2919.

——, and A. C. Hirst, 1989: Interannual variability in a tropical atmosphere–ocean model: Influence of the basic state, ocean geometry and nonlinearity. *J. Atmos. Sci.*, **46,** 1687–1712.

Bigg, G. R., and J. R. Blundell, 1989: The equatorial Pacific ocean prior to and during El Niño of 1982–83—a normal mode model view. *Quart. J. Roy. Meteor. Soc.*, **115,** 1039–1069.

Busalacchi, A. J., and J. J. O'Brien, 1981: Interannual variability of the equatorial Pacific in the 1960s. *J. Geophys. Res.*, **86,** 10 901–10 907.

——, K. Takeuchi and J. J. O'Brien, 1983: Interannual variability of the equatorial Pacific-revisited. *J. Geophys. Res.*, **88,** 7551–7562.

Cane, M. A., and E. S. Sarachik, 1981: The response of a linear baroclinic equatorial ocean to periodic forcing. *J. Mar. Res.*, **39,** 651–693.

——, and R. J. Patton, 1984: A numerical model for low-frequency equatorial dynamics. *J. Phys. Oceanogr.*, **14,** 1853–1863.

Gill, A. E., 1980: Some simple solutions for heat-induced tropical circulation. *Quart. J. Roy. Meteor. Soc.*, **106,** 447–462.

——, 1981: An estimation of sea level and surface current anomalies during the 1972 El Niño and consequent thermal effect. *J. Phys. Oceanogr.*, **13,** 586–606.

Hirst, A. C., 1988: Slow instabilities in tropical ocean basin–global atmosphere models. *J. Atmos. Sci.*, **45,** 830–852.

Kessler, W. S., 1990: Can reflected extra-equatorial Rossby waves drive ENSO. *J. Phys. Oceanogr.*, **21,** 444–452, (1991).

Kubota, M., and J. J. O'Brien, 1988: Variability of the upper tropical Pacific ocean model. *J. Geophys. Res.*, **93,** 13 930–13 940.

Legler, D. M., and J. J. O'Brien, 1988: Tropical Pacific wind stress analysis for TOGA. *IOC Time Series of Ocean Measurements,* IOC Technical Series 33, Vol. 4, UNESCO.

Schopf, P. S., and Suarez, M. J., 1988: Vacillations in a coupled atmosphere–ocean model. *J. Atmos. Sci.*, **45,** 549–566.

Seager, R., 1989: Modeling tropical Pacific sea surface temperature: 1970–87. *J. Phys. Oceanogr.*, **19,** 419–434.

Suarez, M. J., and P. S. Schopf, 1989: A delayed action oscillator for ENSO. *J. Atmos. Sci.*, **45,** 3283–3287.

White, W. B., G. Meyers, J. R. Donguy and S. Pazan, 1985: Short-term climatic variability in the thermal structure of the Pacific ocean during 1979–82. *J. Phys. Oceanogr.*, **15,** 917–935.

——, Y. He and S. E. Pazan, 1989: Off-equatorial westward propagating waves in the tropical Pacific during the 1982–83 and 1986–87 ENSO events. *J. Phys. Oceanogr.*, **19,** 1397–1406.

Zebiak, S. E., 1989: Oceanic heat content variability and El Niño cycles. *J. Phys. Oceanogr.*, **19,** 475–486.

——, and M. A. Cane, 1987: A model El Niño-Southern Oscillation. *Mon. Wea. Rev.*, **115,** 2262–2278.